Experimental studies on the corrosion inhibition effect of new synthesized pyrazole derivatives on C38 steel in 0.5 M H₂SO₄ and HCl 1M

A. Attou[1,2], A. Benikdes[1,3], O. Benali[1,4], H.B. Ouici[1,2] and A. Guendouzi[1,2]*

[1]*Department of Chemistry, Faculty of Science, University of Saïda, Algeria, [2]Laboratory of Chemistry, Synthesis, Properties and Applications, University of Saïda, Saïda, Algeria and [3]Department of civil engineering and hydraulic, Faculty of Technology, University of Saïda- Algeria.[4]Department of Biology, Faculty of Science, University of Saïda, Algeria*

Abstract

Inhibition of C38 steel corrosion by two pyrazolederivatives in 0.5M H₂SO₄ and 1 M HCl was investigated by weight loss, potentiodynamic polarization and electrochemical impedance spectroscopy (EIS) measurements. The inhibition efficiency increased with increase in inhibitor concentration but deceased with rise in temperature and immersion time. The thermodynamic parameters of corrosion and adsorption processes were determined and discussed. The adsorption of these inhibitors was found to obey Langmuir adsorption isotherm. The results obtained from the three different techniques were in good agreement.

Keywords: Corrosion inhibition; C38 steel; acid solution; pyrazole derivatives

1. Introduction

Generally, acid solutions are used for the removal of rust and scale in industrial processes. It is already known that organic inhibitors are used in these processes to control metal dissolution [1-3]. Most of the well-known inhibitors are the compounds containing N, S, and or O atoms [4-6]. Organic compounds containing functional electronegative groups and π electrons in conjugated form are used which enable them to adsorb to the metal surface and form protective film [7-10]. The study of inhibition of corrosion by organic compounds is an active field of contemporary research [11-13]. In addition, to explain the mechanism of inhibition of corrosion, the computational quantum chemical calculations and molecular simulation studies have been largely used in the relevant field[14-18]. Indeed, the geometry of the inhibitor molecule in its stable state and the nature of their molecular orbitals are directly involved in the inhibitive properties of these molecules [19-20]. The present work is an attempt to explore the corrosion inhibition action of:5-(4-dimethylamino)phenyl)-3-(4-dimethylamino)styryl)-4,5-dihydro-1H-pyrazole-1-carbothioamide (P1) and 5-(4-dimethylamino)phenyl)-3-phenyl-4,5-dihydro-1H-pyrazole-1-carbothioamide (P2) on C38 steel in 1 M HCl and 0.5 M H₂SO₄ by weight loss measurements an electrochemical methods (Tafel polarization and electrochemical impedance spectroscopy). The mechanism of inhibition was ascertained by adsorption and thermodynamic studies. The reactivity of these compounds was analyzed through theoretical calculations based on density functional theory to explain the varied efficiencies of these compounds as corrosion inhibitors.

2. Experimental
2.1. Materials

C38 steel composed of (in wt.%) of 0.370% C, 0.230% Si, 0.680% Mn, 0.016% S, 0.077% Cr, 0.011% Ti, 0.059% Ni, 0.009% Co, 0.160% Cu, and the remainder iron (Fe) was used as the working electrode for all studies. Inhibitors were synthesized in the laboratory and were purified and analyzed by IR and NMR spectroscopies before use. Figure 1 shows the molecular structures of the investigated organic compounds which have been labeled P1 and P2.
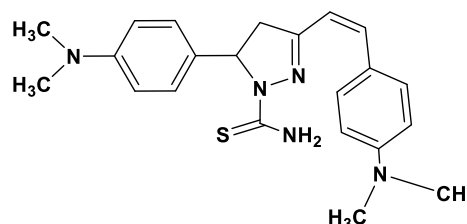
P1: 5-(4-dimethylamino)phenyl)-3-(4-dimethylamino)styryl)-4,5-dihydro-1H-pyrazole-1-carbothioamide
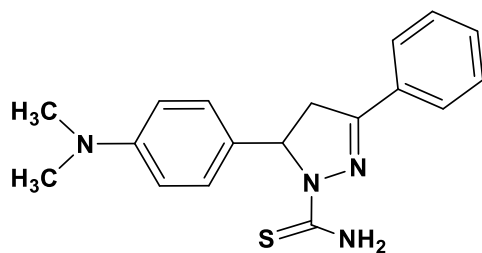
P2: 5-(4-dimethylamino)phenyl)-3-phenyl-4,5-dihydro-1H-pyrazole-1-carbothioamide

Figure 1: Structure of P1 and P2

The acid solutions were made from AR grade H_2SO_4 and HCl. Appropriate concentration of acid was prepared by using distilled water.

2.2. Weight loss measurements

For the weight loss measurements, the experimentswere carried out in solution of 0.5 M H_2SO_4 and 1 M HCl (uninhibited and inhibited) on C38 steel. Sheets with dimensions 3×1×0.2 cm were used. They were polished successively with different grades (400 to 1000). Each run was carried out in a glass vessel containing 50 ml test solution. A clean weight C38 steel sample was completely immersed at an inclined position in the vessel. After 1 h of immersion in both acids with and without addition of inhibitor at different concentrations, the specimen was withdrawn, rinsed with distilled water, washed with acetone, dried and weighted. The weight loss was used to calculate the corrosion rate inmilligrams per square centimeter per hour.

2.3. Electrochemical measurements

Electrochemical experiments were carried out in a glass cell (CEC/TH-Radiometer) with a capacity of 500 ml. A platinum electrode and a saturated calomel electrode (SCE) were used as a counter electrode and a reference electrode. The working electrode (WE) was in the form of a disc cut from mild steel under investigation and was embedded in a Teflon rod with an exposed area of 1 cm^2.Potentiodynamic polarization and electrochemical impedance spectroscopy (EIS) were conducted in an electrochemical measurement system (VoltaLab40) which comprises a PGZ301 potentiostat, a personal computer and VoltaMaster 4 and Zview software. The potentiodynamic current–potential curves were recorded by changing the electrode potential automatically from –700 to –250 mV with scanning rate of 0.5 mV s^{-1}.The ac impedance measurements were performed at corrosion potentials (E_{corr}) over a frequency range of 10 kHz–100 mHz, with a signal amplitude perturbation of 10 mV. Nyquist plots were obtained.

The calculation methods of the electrochemical parameters and inhibition efficiencies are given in our previous work [12-13].

3. Results and discussion

3.1. Weight loss studies

3.1.1 Effect of concentration

Table 1 shows the values of the corrosion rate and inhibition efficiency obtained from the weight loss measurements of C38 steel for different concentrations of P1 and P2 in 0.5 M H_2SO_4 and 1M HCl at 30˚C after 1 h of immersion.Corrosion rate (C_R) and inhibition efficiency (IE_W) were calculated using the following formula:

$$CR=\Delta W/S.t \quad (1)$$

$$IE_W(\%)=(CR_a-CR_p)/CR_a.100 \quad (2)$$

where, ΔW is the weight loss, S is the surface area of the specimen (cm^2), t is the immersion time (h), CR_a and CR_p are corrosion rates in the absence and presence of the inhibitor, respectively.

Table 1: Corrosion rate of C38 steel and inhibition efficiency for various concentrations of P1 and P2 for the corrosion of C38 steel in 0.5 M H_2SO_4 and HCl 1M at 30˚C

		Conc. (M)	C.R (mg cm^{-2} h^{-1})	IE_W (%)
P1	0.5 M H_2SO_4	Blank	6.43	----
		10^{-6}	2.835	55.95
		5×10^{-6}	1.75	72.80
		10^{-5}	1.39	78.39
		5×10^{-5}	0.245	96.19
	1 M HCl	Blank	0.980	----
		10^{-6}	0.45	54.08
		5×10^{-6}	0.305	68.88
		10^{-5}	0.251	78.57
		5×10^{-5}	0.165	83.16
		10^{-4}	0.13	86.73
P2	0.5 M H_2SO_4	Blank	6.43	----
		10^{-6}	3.67	43.58
		10^{-5}	1.87	70.94
		10^{-4}	0.165	97.44
	1 M HCl	Blank	0.980	----
		10^{-6}	0.26	73.47
		10^{-5}	0.195	80.10
		10^{-4}	0.165	83.16

From this table we can see that the inhibition efficiency increases with concentration in both acids. It is a noted that this phenomenon may be attributed to increase in number of molecules occupied by the inhibitor on the C38 steel–acid solution interface. As the number of molecules increases, the corrosion reactions are prevented from occurring over the active sites of the C38 steel surface covered by adsorbed inhibitor species, whereas the corrosion takes place on the surface not covered by the inhibitor molecules [21-22]. The results obtained show that the inhibitors exhibited a higher inhibiting effect on C38 steel in the order H_2SO_4 >HCl. This

indicates that the degree of protonation as well as nature of the acid anions influence the corrosion process [23]. As a comparison between the two inhibitory molecules P1 and P2, it is clearly stated that the product P1 is significantly better than the product P2 whether in HCl or H_2SO_4. This may be due to the presence of a supplementary double bond as well as the presence of an amine function in the phenyl group.

3.1.2 Effect of immersion time

Table 2 illustrates results of evaluated inhibition efficiency of the inhibitor at 5×10^{-5} M in H_2SO_4 at various immersion periods. From this table, it can be seen that the inhibition efficiency decreases slightly after 480 min (6 hours) of immersion but this decrease becomes more important after immersion of 1440 min (24 hours). This finding leaves us thinking that the use of this inhibitor is preferable for low immersion times. This phenomenon can be explained by the relaxation of the film formed by the inhibitory molecules with the immersion time.

Table 2: Variation of the inhibition efficiency versus the immersion time for the optimal concentration at 30˚C

Immersion time (min)	IE_w (%)
60	95.64
480	94.95
1440	79.58

3.1.3. Thermodynamic consideration

Temperature is an important kinetic factor of influencing the corrosion rate of steel in acid solutions and the adsorption behaviors of inhibitor on steel surface. In this study, evaluation experiments were conducted to analyze the effect of temperature on the inhibition characteristics. Meanwhile, the effect of temperature on inhibition efficiency (IE_W(%)) and corrosion rate (C.R) obtaining by weight loss measurement for the two compounds in H_2SO_4 0.5M are shown in table 3.

Table 3: Effect of temperature on the corrosion rate and inhibition efficiency of the C38 steel with and without P1 and P2

	Temp. (K)	C.R (mg.cm^{-2}.h^{-1})	IE_w (%)
Blank (0.5 M H_2SO_4)	298	3.14	----
	308	6.43	----
	313	9.58	----
	318	12.62	----
P1 (5.10^{-5} M)	298	0.40	87,12
	308	0.24	96,19
	313	0.86	90,98
	318	0.89	92,95
P2 (10^{-4} M)	298	0.12	96.18
	308	0.16	97.33

313	0.34	96.4
318	0.62	95.07

From this table it is clearly seen that the values of corrosion rates increase with increasing temperatures in the presence or in the absence of the two inhibitors (P1 and P2).It should be noted in this context that the method of calculating the activation energies as well as the two other activation parameters (ΔHa and ΔSa) is well detailed in our work than previous works[12-13].The plot of Ln Vcorr vs. 1/T and Ln (Vcorr/T) vs. 1/T of the two compounds at the optimal concentrations and blank is given in figures 2 and 3.
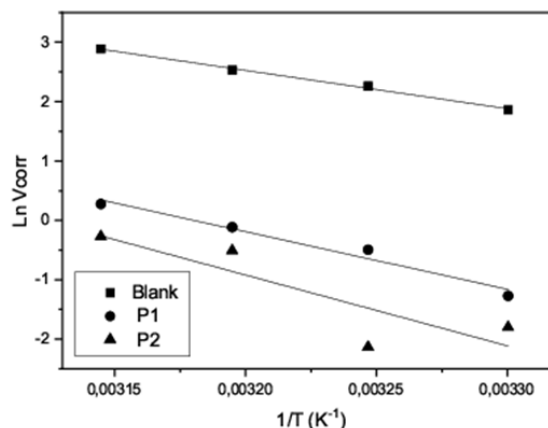

Figure 2: Arrhenius plot of corrosion rate of C38 steel in 0.5 M H_2SO_4 solution in absence and presence of P1 and P2
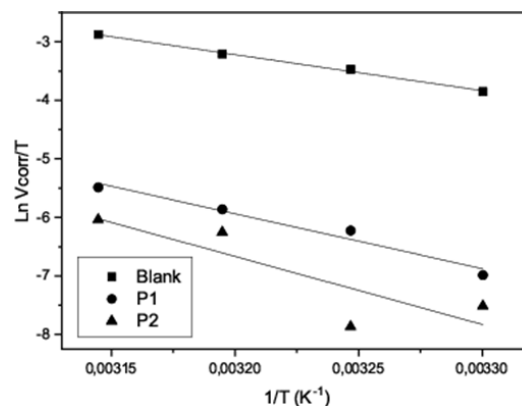

Figure 3: Transition plot of Ln (Vcorr/T) Vs 1/T in 0.5 M H_2SO_4 solution in absence and presence of inhibitors (P1 and P2)

The calculated values of activation energy (Ea) and thermodynamic data such as the enthalpy of adsorption (ΔHa) and the entropy of adsorption (ΔSa) for C38 steel in 0.5 M H_2SO_4 with and without P1 and P2 are listed in Table 4.

Table 4: Activation parameters of dissolution reaction of C38 steel in 0.5 M H_2SO_4 containing optimal concentration of P1 and P2

Conc. (M)	lnA	E_a (kJ mol^{-}	ΔH_a (kJ mol^{-}	ΔS_a (J mol^{-}

		¹)	¹)	¹K⁻¹)
Blank	23.19	53.69	51.11	-60.75
P1 (5×10⁻⁵M)	30.82	80.56	78.01	2.72
P2 (10⁻⁴M)	37.25	99.18	96.60	56.14

Blank (1 M HCl)	308	1,051	----
	313	1,14	----
	318	1,42	----
P1 (5.10⁻⁵ M)	303	0.130	86.73
	308	0.180	82.87
	313	0.252	77.89
	318	0.355	75.00
P1 (5.10⁻⁵ M)	303	0.165	83.16
	308	0.32	69.55
	313	0.63	44.73
	318	0.76	46.47

From Table 3, it is evident that the E_a values and pre-exponential factor are higher in the presence of inhibitors compared to blank. Anusuya et al. [24] attributed, this phenomenon to physical adsorption, where chemical adsorption is more pronounced in the opposite case. On the other hand, the relationship between temperature, percentage inhibition efficiency and E_a in the presence of inhibitors is as follows [24-25]:

(i) For inhibitors, whose percentage inhibition efficiency decreases with increase in T, E_a will be greater than blank.

(ii) For inhibitors, whose percentage inhibition efficiency does not change with temperature, Ea will not change in presence or absence of inhibitors.

(iii) For inhibitors, whose percentage inhibition efficiency increases with increase in temperature, the value of Ea will be less in inhibited solutions compared to uninhibited solutions.

As adsorption decreases more desorption of inhibitor molecules occur because these two opposite processes are in equilibrium. Due to more desorption of inhibitor molecules at higher temperatures, greater surface area of mild steel comes in contact with aggressive environment resulting in an increase in corrosion rates with temperature. The increase in E_a values confirms stronger physiosorption of the inhibitors on the C38 steel surface. Physiosorption is small but important because it is the preceding stage of chemisorption [26]. Fouda et al. [27] interprets that the increase in E_a with increase inhibitor concentration is typical of physical adsorption and the positive signs of the enthalpies (ΔH_a) reflect the endothermic nature of the brass dissolution process. Value of entropies (ΔS_a) imply that the activated complex at the rate determining step represents an association rather than a dissociation step, meaning that a decrease in disordering takes place on going from reactants to the activated complex [28].

In the same way as above, the same tests were carried out in 1M HCl with the two compounds (P1 and P2) for their optimal concentrations and at different temperatures. The obtained results are given in table 5.

Table 5: Effect of temperature on the corrosion rate and inhibition efficiency of the C38 steel with and without P1 and P2

	Temp. (K)	C.R (mg.cm⁻².h⁻¹)	IE$_W$ (%)
	303	0,98	----

From these results we can clearly see that there is a decrease in inhibition efficiency values with rise in temperature and which be interpreted by a physically adsorption (low energy bonds) of inhibitor molecules on the metal surface under study [13]. The plots of ln(Vcorr) against (1/T) for C38 steel corrosion in 1 M HCl in the absence and presence of optimal concentrations of P1 and P2 are given in Figures 4. Apparent activation energy, ΔHa and ΔSa values in the absence and presence of P1 and P2 at different temperatures were calculated from ln(Vcorr) vs. (1/T) plots (Figure 5) are given in Table 6.
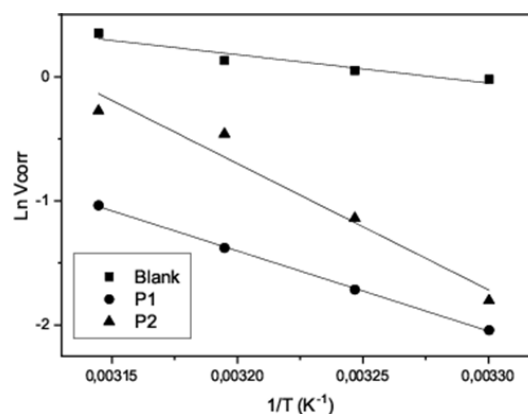

Figure 4: Arrhenius plot of corrosion rate of C38 steel in 0.5 M H₂SO₄ solution in absence and presence of P1 and P2
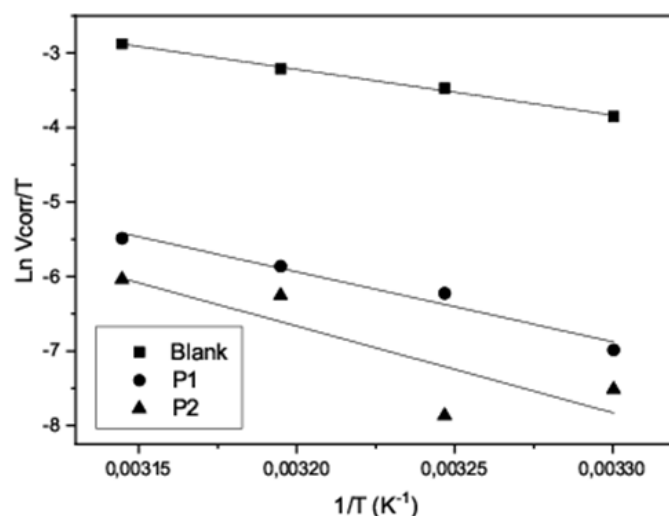

Figure 5: Transition plot of Ln (Vcorr/T) Vs 1/T in 1 M HCl solution in absence and presence of inhibitors (P1 and P2)

Table 6: Activation parameters of dissolution reaction of C38 steel in 1 M HCl containing optimal concentration of P1 and P2

Conc. (M)	lnA	E_a (kJ mol^{-1})	ΔH_a (kJ mol^{-1})	ΔS_a (J mol^{-1}K^{-1})
Blank	7.51	19.05	16.47	-191.13
P1 (5×10^{-5}M)	19.25	53.66	51.08	93.51
P2 (10^{-4}M)	31.82	84.50	81.92	11.02

Table 3 showed that the values of E_a determined in 1 M HCl containing P1 and P2 are higher than that for uninhibited solution. The increase in the apparent activation energy may be interpreted as physical adsorption that occurs in the first stage [29]. All estimated kinetic-thermodynamic parameters were tabulated also in Table 3. Inspection of these data revealed that the thermodynamic parameters (ΔH_a and ΔS_a) for dissolution reaction of C38 steel in 1 M HCl in the presence of both inhibitors are higher than that of in the absence of inhibitors. The positive signs of ΔH_a reflect the endothermic nature of the steel dissolution process suggesting that the dissolution of steel is slow in the presence of inhibitors [30]. One can notice that E_a and ΔH_a values vary in the same way for both inhibitors (Tables 4 and 6). The values of ΔS_a were negative in the absence of inhibitors, implying that the activated complex represented the rate-determining step with respect to the association rather than the dissociation step. It means that a decrease in disorder occurred when proceeding from the reactants to the activated complex [31].

3.1.4. Adsorption consideration

Assuming that, the corrosion inhibition was caused by the adsorption of the tested compounds (P1 and P2), and the values of surface coverage for different concentrations of the inhibitors in 0.5M H$_2$SO$_4$ and 1M HCl were evaluated from weight loss and it was observed that θ values increased with increasing the concentration of the two compounds. The establishment of adsorption isotherm indicates the nature of the metal–inhibitor interaction. For the current study, attempts were made to fit the adsorption data with various isotherms such as Langmuir, Freundlich and Temkin adsorption isotherms. The formulas and methods for calculating thermodynamic parameters have been well described in our previous work [5, 12-13].

Figures 6a and 6b show the Langmuir adsorption isotherm for the P1 and P2. Both linear correlation coefficient (R^2) and slope are close to 1 (Table 7), indicating the adsorption of the two compounds (P1 and P2) on mild steel surface obeys the Langmuir adsorption isotherm in 0.5 M H$_2$SO$_4$ and 1 M HCl solutions.
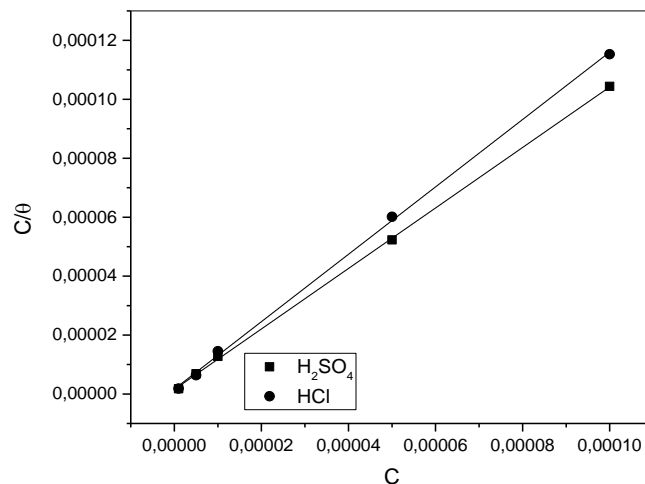

Figure 6a: Langmuir isotherm adsorption model of P1 on the C38 steel surface in 0.5 M H$_2$SO$_4$ and 1 M HCl at 303 K
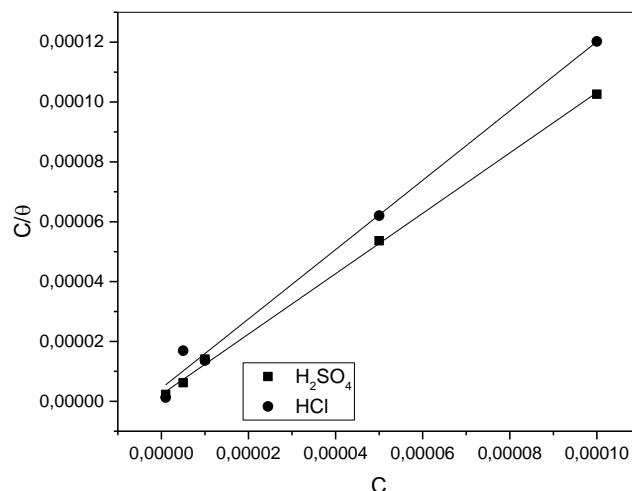

Figure 6b: Langmuir isotherm adsorption model of P2 on the C38 steel surface in 0.5 M H$_2$SO$_4$ and 1 M HCl at 303 K

Table 7: Adsorption parameters for P1 in 0.5 M H$_2$SO$_4$ and 1M HCl obtained from Langmuir adsorption isotherm at 303 K

		R^2	Slope	K_{ads} (L mol^{-1})	ΔG°_{ads} (kJ mol^{-1})
P1	0.5 M H$_2$SO$_4$	0.999	1.02	6.50×10^5	-43.84
	1 M HCl	0.999	1.14	6.01×10^5	-43.64
P2	0.5 M H$_2$SO$_4$	0,999	1.01	4.41×10^5	-42.861
	1 M HCl	0.996	1.16	2.30×10^5	-41.219

In the present study, a large value of K_{ads} was found for the two studied inhibitors indicating the strong adsorption of inhibitor molecules at the surface of C38 steel. The ΔG°_{ads} value calculated in this work indicates that the mechanism of adsorption of inhibitory molecules on the C38 steel surface involves two types of interactions: a predominant

physiosorption and weak chemisorptions [12]. However, and particularly when charged species are adsorbed, it is difficult to distinguish between chemisorption and physisorption only based on these criteria. It should be noted that the possibility of coulombian interactions between adsorbed cations (protonated form of P1 and P2) and specifically adsorbed anions (SO_4^{2-} and Cl^-) can increase Gibbs' energy even if no chemical bond appears [13]. Moreover, the adsorption of the two compounds on anodic sites through lone pairs of electrons of nitrogen, and sulfuric atoms and through π-electrons of phenyl group will then reduce the anodic dissolution of C38 steel [12-13]. From these results, the adsorption process of P2 on the steel surface can be presented as follows in the case of 1M HCl for example (Figure 7).
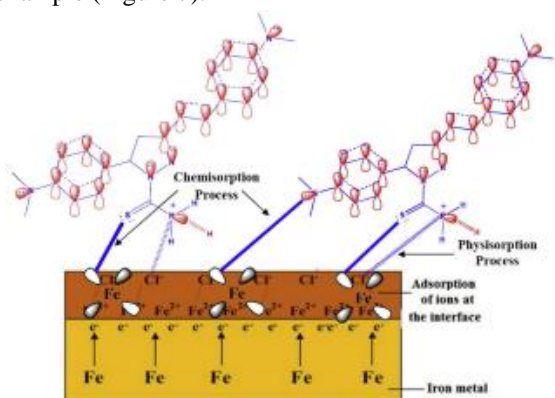

Figure 7: Mechanism of corrosion inhibition of C38 steel in the presence of P1 in 1 M HCl

3.2. Electrochemical measurements

Figure8shows the variation of open circuit potential (E_{OCP}) of C38 working electrodewith immersion time (t) in 0.5M H_2SO_4 in absence and presence of P1 (5×10^{-5} M) and P2 (10^{-4} M) at 303K. For all cases, the initial potential is moved slightly with time, and gradually remains steady value. Meanwhile, it can be observed that after for 12 min immersion, only negligible changes in the $E_{OCP}$are measured. Meanwhile, it can be observed that after for 12 min immersion, only negligible changes in the E_{OCP} are measured. Therefore, the steady-state was achieved after 20 min for electrochemical tests. The EOCP value at 30 min in HCl without inhibitor is -0.495 V (versus SCE). The steady-state potential moves positive after adding P2 and moves negative after adding P1 to the aggressive solutions.
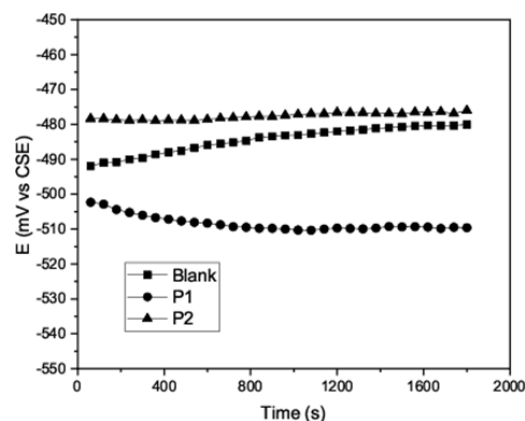

Figure 8: Open circuit potential-time curves for C38 steel in 0.5 M H_2SO_4 in the absence and presence of P1 and P2

At 303 K, the potentiodynamic polarization curves of mild steel in 0.5 M H_2SO_4in the absence and presence of the optimal concentration of P1 and P2. The electrochemical corrosion parameters including corrosion potential, cathodic Tafel slopes, the corrosion current density and inhibition efficiency are given in Table 8.
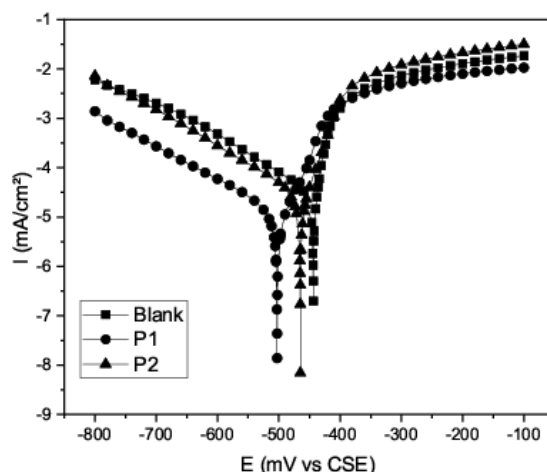

Figure 9: Potentiodynamic polarization curves for C38 steel in 0.5 M H_2SO_4 in the absence and presence of P1 (5×10^{-5}M) and P2 (10^{-4}M) at 303 K

Table 8: The polarization parameters and corresponding inhibition efficiency for C38 steel in 0.5 M H_2SO_4 in the absence and presence of optimal concentrations of P1 and P2 at 303 K

	-Ecorr (mV vs. CSE)	-b$_c$ (mV. Dec^{-1})	I$_{corr}$ (mA.cm^{-2})	E.I$_{Icorr}$ (%)
Blank	423	155	2.34	-----
P2(10^{-4}M)	463	132	$2.88.10^{-2}$	98.76
P1 (5×10^{-5}M)	502	147	$1.25.10^{-2}$	99.46

A decrease in both cathodic and anodic currents is noted [2, 5]. This result shows that the addition of P1 and P2 inhibitor reduces anodic dissolution and also retards the hydrogen

evolution reaction [12]. It can be seen from table 8, that the I_{corr} values decrease with the inhibitors concentration and the addition of the two inhibitors produces slight changes in the values of E_{corr} and b_c. This indicates that the adsorbed molecules of P1 and P2 do not affect the mechanism of hydrogen evolution[6].
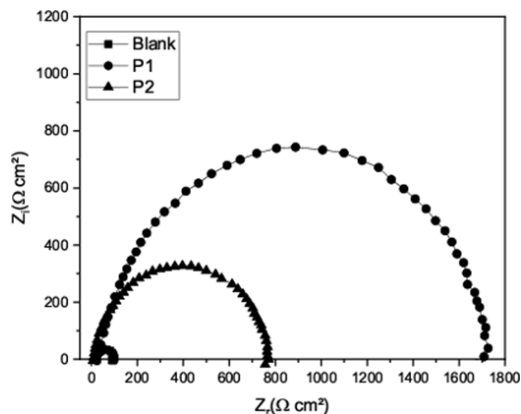

Figure 10: Shows the Nyquist diagrams of C38 steel in 0.5 M H_2SO_4 with the optimal concentrations of P1 (5×10^{-5}M) and P2 (10^{-4}M) at 303 K

The double layer capacitance (C_{dl}), charge transfer resistance (R_{ct}) and corresponding inhibition efficiency ($I.E_{Rt}(\%)$) obtained from electrochemical impedance spectroscopy (EIS) is presented in table 9.It can be found that all Nyquist plots show a single capacitive loop, in both uninhibited and inhibited solutions, which is attributed to the charge transfer of corrosion process [12-13]. The impedance spectra show that the single semicircle and the diameter of semicircle increase in the presence of P1 and P2.

Table 9: Impedance parameters and inhibition efficiency for the corrosion ofC38 steel in 0.5 M H_2SO_4 containing the optimal concentration of P1 and P2 at 303 K

C_{inh} (M)	R_t (Ωcm^2)	$Q \times 10^4$ ($s^n\Omega^{-1}cm^{-2}$)	N	C_{dl} ($\mu F\ cm^{-2}$)	$I.E_{Rt}$ (%)
Blank	73.26	3.06	0.89	161.43	----
P2 (10^{-4}M)	749.4	1.32	0.89	90.56	90.22
P1 (5×10^{-5}M)	1652.12	1.90	0.89	123.28	95.56

It can be seen from table 9 that, the presence of the two compounds enhances the values of R_t and reduces the C_{dl} values. The decrease in C_{dl} may be due to the adsorption of P1 and P2 to form an adherent film on the metal surface and suggests that the coverage of the metal surface with this film increases the double layer thickness [1-2, 5].The results obtained from EIS are in good agreement with the results obtained from potentiodynamic polarization and weight loss measurement.

4. Conclusions

We can deduce from the overall experimental results the following conclusions:

- The investigated compounds are good inhibitors for C38 steel corrosion in 0.5M H_2SO_4 and 1 M HCl.
- The order of %IE of these investigated compounds is in the following order: P1>P2.
- The results obtained from all weight loss measurements showed that the inhibiting action increases with the inhibitor concentration and decreases with raising immersion time and the temperature.
- When the inhibitor is added the double layer capacitances decrease with respect to blank solution. This fact confirms the adsorption of P1 and P2 on the C38 steel surface.
- The thermodynamic parameters revealed that the inhibition of corrosion by investigated compounds is due to theformation of a physical and or chemical adsorbed film on the metal surface, and the adsorption of inhibitor on C38 surface follows Langmuir isotherm for these compounds.
- Reasonably good agreement was observed between the values of IE obtained by the weight loss and electrochemical measurements.

References

[1] H.B. Ouici, M. Belkhouda, O. Benali, R. Salghi, L. Bammou, A. Zarrouk and B. Hammouti. (2015). Adsorption and inhibition effect of 5-phenyl-1, 2, 4-triazole-3-thione on C38 steel corrosion in 1 M HCl. Res. Chem. Intermed. 41: 4617-4634.

[2] H.B. Ouici, O. Benali and A. Guendouzi (2015): Corrosion Inhibition of Mild Steel in Acidic Media Using Newly Synthesized Heterocyclic Organic Molecules: Correlation between Inhibition Efficiency and Chemical Structure. AIP Publishing. 020086.

[3] I.I. Bergmann, Corrosion Inhibitors (1963) Macemillan, New York. Pp.126-153.

[4] Y.I. Kuznetsov. (1996). Organic Inhibitors of Corrosion of Metals, Springer US, p.282.

[5] M. Zebida, O. Benali, U. Maschke and M. Trainsel. (2019). Corrosion inhibition properties of 4-methyl-2-(methylthio)-3-phenylthiazol-3-ium iodide on the carbon steel in sulfuric acid medium, Inter. J. Corr. Scale Inhib. 8 (3): 613-627.

[6] A.A. Farag, M.A. Migahed and E.A. Badr. (2019). Thiazole Ionic Liquid as Corrosion Inhibitor of Steel in 1M HCl Solution: Gravimetrical, Electrochemical, and Theoretical Studies. J Bio Tribo Corros.5:53.

[7] T.A. Salman, D.S. Zinad, S.H. Jaber, M.Al-Ghezi, A. Mahal, M. Takriffand A.A. Al-Amiery. (2019). Effect of 1,3,4-Thiadiazole Scaffold on the

Corrosion Inhibition of Mild Steel in Acidic Medium: An Experimental and Computational Study. J. Bio. Tribo. Corros. 5:48.

[8] S.B. Al-Baghdadi, F.T.M. Noori, W.K. Ahmed and A.A. Al-Amiery. (2016). Thiadiazole as a Potential Corrosion Inhibitor for Mild Steel in 1 M HCl. J. Advanc. Electrochem. 2(1): 67–69.

[9] M. Guzmán, R. Lara and L. Vera. (2009). 5-amino-1,3,4-thiadiazole-2-thiol corrosion current density and adsorption thermodynamics on ASTM A-890-1B stainless steel in a 3.5% NaCl solution. J. Chill. Chem. Soc. 54 (2) 123-128.

[10] A. Benikdes, O. Benali, A. Tidjani, M. Tourabi, H. Ouici and F. Bentiss. (2017) Inhibition corrosion of ductile iron by thiadiazol-thiol derivative. J. Mater. Environm. Sci. 8(9): 3175-3183

[11] I. Ahamad, R. Prasad and M.A. Quraishi (2010) Inhibition of mild steel corrosion in acid solution by Pheniramine drug: Experimental and theoretical study. Corros. Sci. 52: 3033–3041.

[12] H. Ouici, M. Tourabi, O. Benali, C. Selles, C. Jama, A. Zarrouk and F. Bentiss. (2017) Adsorption and corrosion inhibition properties of 5-amino 1,3,4-thiadiazole-2-thiol on the mild steel in hydrochloric acid medium: Thermodynamic, surface and electrochemical studies, J. Electroanal. Chem. 803: 125–134.

[13] F. Boudjellal, H.B. Ouici, A. Guendouzi, O. Benali and A. Sehmi (2020) Experimental and theoretical approach to the corrosion inhibition of mild steel in acid medium by a newly synthesized pyrazole carbothioamide heterocycle, J. Mol. Struc. 1199: 127051.

[14] H.B. Ouici, O. Benali and A. Guendouzi (2016) Experimental and quantum chemicalstudies on the corrosion inhibition effect of synthesized pyrazole derivatives on mild steel in hydrochloric acid, Res. Chem. Intermed. 42: 7085-7109.

[15] F. El-Taib Heakal, S.K. Attia, S.A. Rizk, M.A. Abou Essa and A.E. Elkholy (2017) Synthesis,characterization and computational chemical study of novel pyrazole derivatives as anticorrosion and antiscalant agents, J. Mol. Struct. 1147: 714-724.

[16] R.A. Gupta and S.G. Kaskhedikar (2013) Synthesis, anti-tubercular activity, and QSAR analysis of substituted nitroaryl analogs: chalcone, pyrazole, isoxazole, and pyrimidines. Med. Chem. Res. 22: 3863-3880.

[17] A.M. Farag, N.A. Kheder, K.M. Dawood and A.M. El Defrawy. (2017). A facile access and computational studies of new 4,5-biprazole derivatives, Heterocycles 94: 1245-1256.

[18] M. Lebrini, M. Traisnel, M. Lagrenée, B. Mernari and F. Bentiss. (2008). Inhibitive properties, adsorption and a theoretical study of 3,5-bis (n-pyridyl)-4-amino-1,2,4-triazoles as corrosion inhibitors for mild steel in perchloric acid, Corros. Sci. 50: 473-479.

[19] S. B. Al-Baghdadi, F. G. Hashim, A. Q. Salam, T. K. Abed, T. S. Gaaz, A. A. Al-Amiery, A. A. H. Kadhum, K. S. Reda and Wahab K.Ahmed. (2018). Synthesis and corrosion inhibition application of NATN on mild steel surface in acidic media complemented with DFT studies, Results in Physics, 8: 1178-1184.

[20] H. Ashassi-Sorkhabi, S. Moradi-Alavian, M.D. Esrafili and A. Kazempour. (2019). Hybrid sol-gel coatings based on silanes-amino acids for corrosion protection of AZ91 magnesium alloy: electrochemical and DFT insights. Prog. Org. Coat. 131: 191-202.

[21] M. Lashgari, M.R. Arshadi and M. J. Biglar (2010) Experimental and theoretical studies of media effects on copper corrosion in acidic environments containing 2-amino-5-mercapto-1,3,4-thiadiazole, Iran. Chem. Soc. 7: 478-486.

[22] M. Lagrenée, B. Mernari, M. Bouanis, M. Traisnel and F. Bentiss (2002). Study of the mechanism and inhibiting efficiency of 3,5-bis(4-methylthiophenyl)-4H-1,2,4-triazole on mild steel corrosion in acidic media. Corros Sci. 44 (3): 573-588.

[23] J. Saranya, P. Sounthari and S. Chitra. (2017). Comparison of the inhibition property of Quinoxaline derivative on mild steel in 1.5M H_2SO_4, 3M HCl and 1M H_3PO_4, J. Mater. Environm. Sci. 8(1): 370-377.

[24] N. Anusuya, P. Sounthari, J. Saranya, K. Parameswari and S. Chitra (2015) Corrosion inhibition effect of hydroxy pyrazoline derivatives on mild steel in sulphuric acid solution together with Quantum chemical studies, J. Mater. Environ. Sci. 6 (6): 1606-1623.

[25] Qu Q., S. Jiang, W. Bai and L. Li (2007) Effect of ethylenediamine tetraacetic acid disodium on the corrosion of cold rolled steel in the presence of benzotriazole in hydrochloric acid. Electrochim. Acta. 52: 6811-6820.

[26] Herrag L., B. Hammouti, S. Elkadiri, A. Aoumt, C. Jama, H. Vezin and F. Bentiss. (2010) Adsorption properties and inhibition of mild steel corrosion in hydrochloric solution by some newly synthesized diamine derivatives: Experimental and theoretical investigations Corros. Sci., 52 (9): 3042.

[27] A.S. Fouda, K. Shalabi and R. Ezzat (2015) Evaluation of some thiadiazole derivatives as acid corrosion inhibitors for, carbon steel in aqueous solutions, J. Mater. Environ. Sci. 6 (4): 1022-1039

[28] A. A. Aksut, W. J. L. Lorenz and F. Mansfeld. (1982). The determination of corrosion rates by electrochemical d.c. and a.c. methods—II. Systems with discontinuous steady state polarization behavior.Corros.Sci. 22 (7): 611-619.

[29] S. Martinez and I. Stern. (2002). Thermodynamic characterization of metal dissolution and inhibitor adsorption processes in the low carbon steel/mimosa tannin/sulfuric acid system. Appl. Surf. Sci. 199 (1–4): 83–89.

[30] N. M. Guan, L. Xueming, and L. Fei. (2004). Synergistic inhibition between o-phenanthroline and chloride ion on cold rolled steel corrosion in phosphoric acid, Mater. Chem. Phys. 86 (1): 59–68.

[31] T. Szauer and A. Brand. (1981). Mechanism of inhibition of electrode reactions at high surface coverages—II, Electrochim. Acta, 26(9): 1219–1224.